Advanced Ceramics Progress: Vol. 11, No. 3, (Summer 2025) 39-51

Materials and Energy Research Center
MERC

Contents lists available at ACERP

Advanced Ceramics Progress

Journal Homepage: www.acerp.ir

Original Research Article

Evaluating in Vitro Calcium Phosphate Formation on the Surfaces of Synthesized Silanated Polymethylmethacrylate Microspheres

Fatemeh Mohammadi [a], Saeed Hesaraki [b]*, Rahim Naghizadeh [c], Nader Nezafati [d], Mojtaba Beygzadeh [e]

[a] MSc Student, School of Materials and Metallurgical Engineering, Iran University of Science and Technology, Tehran, Iran.
[b] Professor, Department of Nanotechnology and Advanced Materials, Materials and Energy Research Center, Karaj, Iran.
[c] Associate Professor, School of Materials and Metallurgical Engineering, Iran University of Science and Technology, Tehran, Iran.
[d] Associate Professor, Department of Nanotechnology and Advanced Materials, Materials and Energy Research Center, Karaj, Iran.
[e] Assistant Professor, Department of Energy, Materials and Energy Research Center, Karaj, Iran.

*Corresponding Author Email: s-hesaraki@merc.ac.ir.ac.ir (S. Hesaraki)
URL: https://www.acerp.ir/article_244974.html

ARTICLE INFO

Article History:
Received 02 August 2025
Received in revised form 11 September 2025
Accepted 16 November 2025

Keywords:
Polymethyl Methacrylate,
Y-Glycidoxypropyltrimethoxysilane,
Tetraethylorthosilcate,
Simulated Body Fluid,
Bioactivity

ABSTRACT

Poly(methyl methacrylate) (PMMA) bone cement is widely used in orthopedic applications such as kyphoplasty and prosthesis fixation due to its favorable mechanical properties. However, its inherent bioinertness limits direct bonding with bone tissue. This study presents a novel approach to enhance the bioactivity of PMMA through surface chemical modification of the powder phase. PMMA microspheres were synthesized using the solvent evaporation emulsification method, which involved optimizing the surfactant type and concentration, as well as process parameters, to achieve morphological stability. Surface hydrolysis with sulfuric acid was conducted to introduce carboxylic functional groups. Subsequently, chemical functionalization was performed using varying concentrations of silane coupling agents, GPTMS and TEOS. FTIR spectroscopy and SEM analyses confirmed successful surface modification while preserving microsphere morphology. Bioactivity was evaluated by immersing the samples in simulated body fluid (SBF) for 1, 7, and 14 days. A gradual formation of a hydroxyapatite layer was observed on the modified surfaces, as evidenced by SEM imaging, FTIR spectra, and XRD patterns. The results demonstrate that surface silanization considerably improves the bioactivity of PMMA microspheres. This surface modification strategy shows strong potential for developing PMMA-based implant materials with enhanced osseointegration capability.

https://doi.org/10.30501/acp.2025.538730.1182

1. INTRODUCTION

Bone is a vital tissue responsible for providing structural support, protecting internal organs, and storing minerals (Clarke, 2008). In cases such as fractures, osteoporosis, or tumor-induced bone loss, natural healing is often insufficient, necessitating clinical interventions like bone grafts or bone cements (Loi et al., 2016). Poly(methyl methacrylate) (PMMA) has long been used as a bone cement due to its favorable mechanical properties, injectability, and rapid setting. However, its bioinert nature, exothermic polymerization, and release of cytotoxic monomers pose significant clinical limitations. To address these challenges, bioactive fillers and surface modification techniques have been widely investigated (Aquino et al., 2016). In this study, PMMA microspheres were synthesized via solvent evaporation emulsification and subsequently surface-modified using acid hydrolysis followed by silanization with GPTMS and TEOS. These treatments aimed to introduce carboxylic functional groups and enhance interfacial

Please cite this article as: Mohammadi, F., Hesaraki, S., Naghizadeh, R., Nezafati, N. & Beygzadeh, M. (2025). Evaluating in Vitro Calcium Phosphate Formation on the Surfaces of Synthesized Silanated Polymethylmethacrylate Microspheres, *Advanced Ceramics Progress*, 11(3), 39-51. https://doi.org/10.30501/acp.2025.538730.1182

adhesion between the organic and inorganic phases. The success of surface modification was verified through FTIR, EDS, and titration analysis. The modified microspheres demonstrated improved hydrophilicity and surface reactivity, highlighting their potential to enhance the bioactivity of PMMA-based bone cements for orthopedic applications.

2. MATERIALS AND METHODS

2.1. Materials Used

Poly(methyl methacrylate) (PMMA, Mw ≈ 120,000; Sigma-Aldrich) microspheres were synthesized using the solvent evaporation method with dichloromethane (DCM, 99.5%, Mw: 84.93 g/mol; Merck) as the organic solvent and polyvinyl alcohol (PVA, 88% hydrolyzed, Mw: 146–186 kDa) as the stabilizer. Surface functionalization was performed through acid hydrolysis using diluted sulfuric acid (95–97%, Merck) to introduce carboxylic acid (-COOH) groups onto the PMMA surface.

The success of the functionalization was confirmed via back titration using sodium hydroxide (NaOH, Mw: 40.00 g/mol), hydrochloric acid (HCl), and phenolphthalein as an indicator. Subsequently, surface modification was conducted through silanization using (3-glycidyloxypropyl) trimethoxysilane (GPTMS, Mw: 236.34 g/mol) and tetraethyl orthosilicate (TEOS, purity > 98%) in ethanol (99.8%, Mw: 46.07 g/mol), with ammonium hydroxide solution (28% NH_3) serving as a catalyst.

2.2. PMMA Microspheres Synthesis

Two different approaches based on the oil-in-water (O/W) emulsion method were evaluated to synthesize PMMA microspheres, following the procedure reported by Singh et al. (2017). In the first method (PMS1), a solution containing 10 wt% polyvinyl alcohol (PVA) and 0.04 g sodium dodecyl sulfate (SDS) was prepared, and 5 wt% PMMA was added. The mixture was emulsified at 7000 rpm using a mechanical stirrer at room temperature, then stored at 4 °C for 48 h to stabilize the microspheres.

The particles were subsequently collected via centrifugation at 9000 rpm for 20 min. However, due to undesirable morphological changes, this method was excluded from further analysis. In the second approach (PMS2), designed to improve particle morphology and uniformity, SDS was omitted. A 6 wt% PMMA solution was added to a 6 wt% aqueous PVA solution, followed by homogenization at 3000 rpm for 5 min at room temperature.

The emulsion was then stirred for 24 h to ensure complete evaporation of dichloromethane (DCM). The absence of SDS and adjustment of mixing parameters resulted in significantly improved microsphere morphology and size uniformity, making this method more suitable for subsequent functionalization and characterization.

2.3. Surface Functionalization of PMs2 Microspheres

To modify the surface of PMS2 microspheres, an acid hydrolysis process was employed. The hydrolysis was conducted in a strongly acidic medium (pH ≈ 2) using a 30 wt% sulfuric acid (H_2SO_4) solution. PMs2 microspheres (5 wt%) were dispersed in the acidic solution and magnetically stirred at 60 °C for 1 h. This treatment aimed to introduce carboxylic acid (-COOH) functional groups onto the microsphere surface, thereby enhancing their chemical reactivity for subsequent surface functionalization.

2.4. Quantification of carboxylic acid groups by back titration

The number of carboxylic acid groups present on the surface of the F-PMS2 sample was determined using a back titration method. A known amount of the sample (0.03 g) was placed in an Erlenmeyer flask, and 85 mL of sodium hydroxide (NaOH, 8.33 mM) was added from a burette. Phenolphthalein was used as the acid-base indicator, appearing colorless under acidic conditions. To ensure complete reaction between NaOH and the carboxylic acid groups, the suspension was stirred for 24 h at room temperature, followed by centrifugation. The excess unreacted NaOH in the supernatant was then titrated with 8 mM potassium hydrogen phthalate (KHP), a primary standard. The color change of the indicator indicated the reaction endpoint. Based on the volume of KHP consumed, the amount of carboxylic acid groups in the sample was calculated.

2.5. PMMA – Siloxane Microsphere Synthesis

As shown in Table 1, surface silanization of F-PMS2 microspheres was performed to form a silica-based coating. Initially, 0.2 g of F-PMS2 powder was dispersed in 40 mL of ethanol and magnetically stirred at room temperature for 10 min. Subsequently, TEOS and GPTMS were added to a solution containing 3 mL of deionized water and 3 mL of 30 % ammonium hydroxide (NH_4OH), which served as a basic catalyst. To assess the effect of precursor ratios on coating quality, three different molar ratios of GPTMS to TEOS were tested (2:1, 3:2, and 2.5:1.5). The reaction was allowed to proceed under ambient conditions for 48 h. Finally, the silanized microspheres were collected via centrifugation at 8000 rpm for 5 min, washed with ethanol, and dried for subsequent characterization.

TABLE 1. Experimental conditions for surface modification of F-PMs2 microspheres using various GPTMS: TEOS ratios

Sample Code	F-PMs2: Ethanol	H2O: NH4OH	GPTMS: TEOS
PMsG	0.2 : 40	3:3	2 : 0
PMS1G2	0.2 : 40	3 : 3	2 : 1
PMS2G3	0.2 : 40	3 : 3	3 : 2
PMS1.5G2.5	0.2 : 40	3 : 3	2.5 : 1.5

2.6. Formation of Calcium Phosphate Precipitate

The bone-bonding ability of a material is typically evaluated based on its capacity to induce calcium phosphate deposition and its subsequent transformation into hydroxyapatite (HAp) on the surface when immersed in simulated body fluid (SBF), which has ion concentrations nearly equivalent to those of human plasma. To assess the apatite-forming ability of the prepared powders, the samples were immersed in SBF for various periods of up to 14 days. Each powder sample was placed separately in a Petri dish containing 6 mL of SBF and incubated at 37 °C. The SBF solution was refreshed daily. After the designated immersion periods, the powders were removed from the solution, rinsed with distilled water, and dried. The surface morphology and physicochemical properties of the samples after 7 and 14 days of immersion were analyzed using FESEM imaging, EDX analysis, FTIR spectroscopy, and XRD.

2.7. Characterization Methods

2.7.1 Fourier Transform Infrared Spectroscopy (FTIR) Analysis

Fourier Transform Infrared Spectroscopy (FTIR) was employed to identify the functional groups and evaluate the chemical structure of the PMMA-based microspheres. All samples were finely ground, mixed with potassium bromide (KBr) at a 2:100 weight ratio, and pressed into pellets under vacuum. The FTIR spectra were recorded using a VECTOR 33 spectrometer over a wavenumber range of 400 to 4000 cm^{-1} with a resolution of 4 cm^{-1}. This technique enabled the detection of characteristic vibrational modes associated with the functional groups introduced during surface modification.

2.7.2 X-ray Diffraction (XRD) Analysis

X-ray diffraction (XRD) is a non-destructive technique used to identify crystalline phases and analyze the crystal structure of materials. In this study, XRD analysis was conducted using a Philips PW3710 diffractometer with Cu Kα radiation over a 2θ range of 10° to 80° to examine the recovered coatings. The obtained diffraction patterns were analyzed using X'Pert software, and phase identification was carried out based on standard reference data and previous related studies.

2.7.3 Scanning Electron Microscopy (SEM)

Scanning Electron Microscopy (SEM) is a powerful technique used to observe and analyze the surface structures of samples by employing a focused beam of electrons. When the electron beam interacts with the sample surface, the emitted and scattered electrons are detected to produce high-resolution images. This method enables detailed examination of surface morphology, topography, and elemental composition. In this study, the morphology of PMMA microspheres was examined using Field Emission Scanning Electron Microscopy (FESEM) combined with Energy Dispersive X-ray Spectroscopy (EDS) to assess surface features and elemental distribution. Additionally, the diameter of the microspheres was measured from the obtained images using ImageJ software, and the average size was calculated accordingly.

2.7.4 In Vitro Bioactivity Test Using Simulated Body Fluid (SBF)

Simulated Body Fluid (SBF), as proposed by Kokubo, is an ionic solution with a composition closely resembling that of human blood plasma. It is commonly used to evaluate the in vitro bioactivity of bioceramic and bioactive materials. The solution is prepared by dissolving reagent-grade salts—NaCl, $NaHCO_3$, KCl, $K_2HPO_4{\cdot}3H_2O$, $MgCl_2{\cdot}6H_2O$, $CaCl_2$, and Na_2SO_4—in distilled water. The pH is adjusted to 7.2–7.4 using Tris buffer and 1 M HCl. Preparation is conducted at approximately 37 °C to maintain physiological conditions. To prevent precipitation, the order of salt addition is strictly controlled. After preparation, the solution is filtered through a 0.22 μm membrane and stored at 4 °C. SBF is widely employed in bioactivity assessments to evaluate the ability of materials to induce hydroxyapatite (HA) formation on their surface, which is a key indicator of their potential to bond with living bone tissue.

3. RESULT AND DISCUSSION

3.1. Characterization of PMMA Microsphere

3.1.1. Particle Size and Morphology Analysis

In the synthesis of poly(methyl methacrylate) (PMMA) microspheres, optimization of reaction parameters was conducted based on the methodology reported by Mashhadian et al. (2022). Key parameters, including the synthesis method, surfactant type and concentration, temperature, and stirring rate, were critically examined due to their significant influence on the final morphology of the microspheres. Achieving uniform, spherical particles with smooth surfaces and minimal aggregation requires precise control over these variables.

Figure 1(a) illustrates the morphology of PMMA microspheres synthesized via the single emulsion solvent evaporation method. The formation of stable emulsions between two immiscible liquids requires a specific energy input. Therefore, a comparative analysis was performed between a mechanical stirrer and a homogenizer to investigate their effectiveness in producing uniform microspheres. The results indicate that using a homogenizer (Figure 1(b)) provides more uniform and spherical particles due to the higher shear forces and efficient mixing compared to the mechanical stirrer (Figure 1(a)).

As observed in the SEM images, low homogenization speeds (low shear stress) result in relatively consistent particle sizes with narrow distribution. In contrast, at intermediate speeds, particles exposed to higher shear near the homogenizer blade are smaller, while those farther away remain larger due to insufficient energy

input. This highlights the critical role of shear energy in achieving a narrow size distribution and consistent morphology. Additionally, homogenization time is crucial; insufficient duration leads to incomplete droplet breakup, whereas excessive homogenization can deform or rupture microspheres.

Surfactants play a pivotal role in stabilizing emulsions formed by immiscible phases. During solvent evaporation, increasing the viscosity of the system can lead to droplet coalescence. Thus, the type and concentration of surfactant are essential for maintaining emulsion stability. Polyvinyl alcohol (PVA) is widely used for its stabilizing ability, where its hydrophilic portion aligns with the aqueous phase and the hydrophobic tail with the oil phase, thereby stabilizing the droplet interface and preventing aggregation.

To ensure biocompatibility, the microspheres must be fabricated from non-toxic and bioinert polymers. In this process, dichloromethane (DCM), a volatile solvent with a low boiling point (40 °C), is gradually evaporated, increasing the relative concentration of PVA in the aqueous phase. As shown in Figure 1(a), the mechanical stirring method yields heterogeneous particle sizes and frequent agglomeration due to low shear forces, indicating insufficient emulsification. Additionally, the use of SDS as a surfactant results in poor micelle stability and inadequate surface coverage, promoting particle fusion and irregular growth. In contrast, Figure 1(b) demonstrates the formation of well-dispersed, uniform microspheres with smooth surfaces when using a homogenizer. The higher shear forces lead to the breakup of micron- and nanoscale droplets, resulting in a more stable emulsion. The use of PVA also supports uniform solvent evaporation and controlled particle growth. Due to the suboptimal morphology observed in Figure 1(a), samples from this group were excluded from further analysis. All subsequent experiments were conducted using microspheres prepared under the optimized conditions shown in Figure 1(b). SEM image analysis using ImageJ software and histogram plotting in Origin software revealed a near-normal distribution of microsphere sizes, with an average diameter ranging from 14 to 15 µm and a size span of 4 to 21 µm. This relatively narrow and consistent distribution makes the microspheres suitable for biomedical applications such as drug delivery, tissue engineering, and other therapeutic uses.

In a related study by Wang et al. (2020), PMMA microspheres encapsulating the phase change material n-eicosane was synthesized using an emulsion method. Instead of conventional surfactants, cellulose nanocrystals (CNCs) were used to stabilize the droplets, preventing coalescence and ensuring uniform sphere formation. Gradual solvent evaporation yielded solid microspheres with controlled spherical morphology and particle sizes ranging from 5 to 10 µm, suitable for energy storage and controlled release applications.

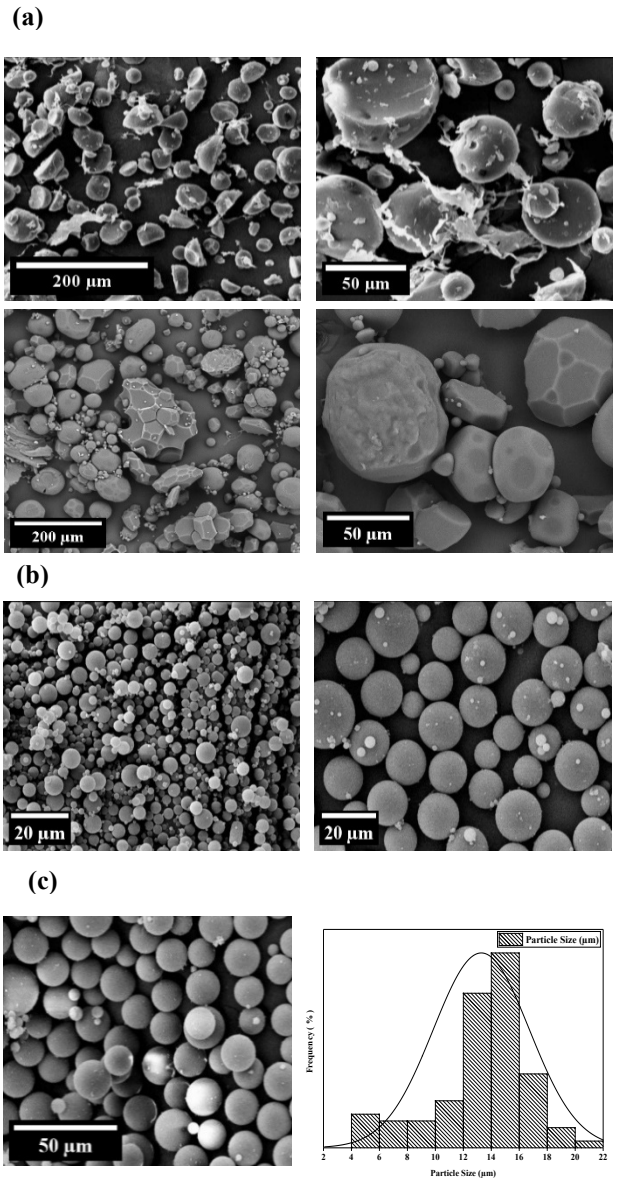

Figure 1. SEM images of microspheres: (a) PMs1 microspheres, (b) PMs2 microspheres, and (c) the corresponding size distribution histogram of PMs microspheres.

3.2 Investigation of Chemical Bonding

3.2.1 Functional Group Modification of Microspheres

Due to the inherently hydrophobic nature of many synthetic or bio-based polymers, chemical surface modification is often essential to render the surface more hydrophilic. This is particularly important because such chemical modifications can introduce strong covalent bonds at the surface, allowing for the stable attachment of various bioactive agents or biomolecules to scaffolds or particulate systems (Teimouri et al., 2023). As illustrated in Figure 2, under acidic conditions and in the presence of protons (H^+ ions), the ester groups

($–COOCH_3$) along the PMMA polymer backbone become protonated, increasing their reactivity. This protonation enhances the susceptibility of the ester bonds to nucleophilic attack by water molecules, promoting ester hydrolysis. As a result, methanol (CH_3OH) and methacrylic acid (MAA) are generated as the primary hydrolysis products (Hosseini et al., 2014). This chemical transformation introduces carboxylic acid (–COOH) functional groups on the microsphere surface, significantly improving surface hydrophilicity and providing reactive sites for subsequent surface functionalization steps, such as silanization or biomolecule conjugation. The generation of –COOH groups is a critical step in tailoring the surface chemistry of PMMA-based materials for biomedical applications, including drug delivery, bone cement modification, and bioactive coating strategies.

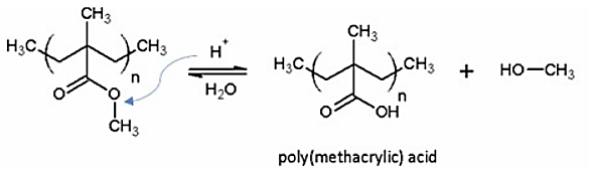

Figure 2. Schematic representation of the mechanism and functional group transformation of PMMA acidic medium.

3.2.2 Determination of Carboxylic Acid Groups by Back Titration

In the modified sample F-PMS2, the ester groups have been converted into carboxylic acid groups (–COOH). Titration is an analytical method used to quantitatively determine the amount of acidic (–COOH) or basic ($–NH_2$) functional groups in a sample. This technique is particularly useful for verifying the successful hydrolysis of ester groups into carboxylic acids in PMMA.

In this method, a pH electrode measures changes in electrical potential as a basic solution, such as sodium hydroxide (NaOH), is gradually added. In the control sample, the titration curve shows no significant change because the ester groups do not participate notably in acid-base reactions. However, in the modified sample, a sudden change in pH is observed, indicating the presence of carboxylic acid groups (–COOH). The amount of NaOH consumed in the modified sample is higher due to the presence of titratable acidic groups.

The experiment aimed to quantify the amount of carboxylic acid groups generated on the surface of the modified PMMA (F-PMS2) compared to the control PMMA sample. Titrations were performed using 8.33 mM NaOH in both samples, with phenolphthalein as the indicator to detect the endpoint.

For PMS2, which lacks titratable carboxylic acid groups, minimal NaOH consumption was expected. Indeed, approximately 10 mL of NaOH was consumed, indicating a negligible amount of acidic functional groups. In contrast, the modified sample consumed about 85 mL of NaOH, a significantly higher volume than the control. After titrating the excess NaOH with 8 mM potassium hydrogen phthalate (KHP), it was found that 30 mL of KHP was consumed, indicating that this volume of NaOH remained unreacted. Therefore, the actual volume of NaOH consumed for neutralizing the acidic groups was 55 mL.

To quantify the amount of carboxylic acid groups formed on the F-PMS2 surface, 85 mL of 8.33 mM NaOH was initially added. Since some of this base reacted with acidic groups and the remainder remained unreacted, the residual NaOH was back-titrated with 8 mM KHP, consuming 30 mL of the solution. By stoichiometric calculation, the amount of unreacted NaOH was 0.24 mmol, while the total added NaOH was 0.708 mmol. Therefore, the amount of NaOH consumed to neutralize the acidic groups was 0.468 mmol.

This result confirms that the surface modification process was successful and that the ester groups were effectively converted into carboxylic acid groups. This chemical change is significant for improving the bioactivity and cell adhesion of PMMA, as the presence of acidic groups enhances interactions with the biological environment and improves its biological performance (Heinrich et al., 2007).

3.2.3 Fourier Transform Infrared (FTIR) Spectroscopy Analysis of Surface Modified and Unmodified PMMA Microspheres

The FTIR spectra of PMMA microspheres (PMs2) and sulfuric acid (6 M) surface-modified microspheres (F-PMs2) were analyzed to investigate the chemical changes induced by surface modification, as shown in Figure 3 (Pahlevanzadeh et al., 2018). Both samples exhibited a characteristic peak around 1730 cm^{-1}, corresponding to the stretching vibration of ester carbonyl groups (C=O) in the PMs2 polymer chain. However, in the F-PMs2 sample, the intensity of this peak showed a slight decrease compared to the control sample, which can be attributed to partial hydrolysis of ester groups and their conversion to carboxylic acid groups (–COOH).

Additionally, a slight increase in absorption was observed in the 3200–3600 cm^{-1} region, corresponding to the stretching vibration of hydroxyl groups (–OH), consistent with the hydrolysis process and the formation of polar groups on the sample surface. Nonetheless, a distinct peak corresponding to carboxylic acid groups (–COOH) was not fully resolved, potentially due to overlap with other vibrational bands or insufficient formation of these groups. It was expected that after acid hydrolysis, a significant increase in the intensity of the –OH peak and a more pronounced decrease in the C=O peak would be observed. However, the data indicate that under the applied conditions, hydrolysis occurred partially and to a limited extent. These results demonstrate that although sulfuric acid surface

modification induced changes in the surface structure, the extent of chemical transformation was insufficient to produce clearly distinguishable new peaks in the FTIR spectra.

According to Pletincx et al. (2017), the initial step of methyl ester hydrolysis (–$COOCH_3$) in PMMA leads to methanol release and conversion to carboxylic acid groups (–COOH). During this process, ATR-FTIR spectra show a decrease in the ester C=O peak (~1732 cm^{-1}), increased absorption in the C–O–C region (~1190 cm^{-1}), and appearance of peaks corresponding to carboxylate groups (~1519–1641 cm^{-1}). These observations align well with the spectral changes noted in our samples and confirm the conversion of the original ester groups to more polar groups (–COOH/COO^-).

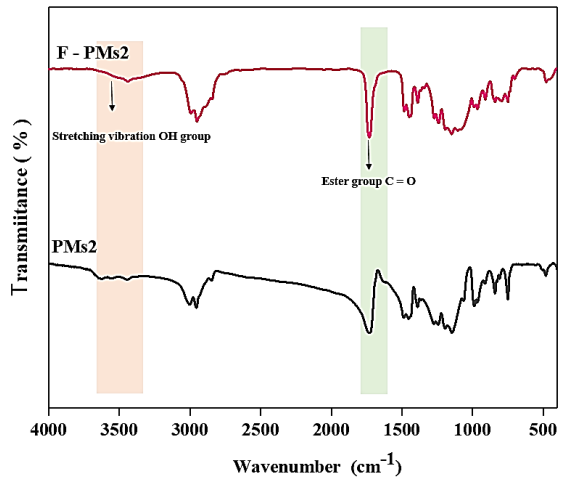

Figure 3. Fourier-transform infrared (FTIR) spectroscopy of PMs2 and F-PMs2 samples.

3.2.4 Chemical Crosslinking Mechanism

The crosslinking between F-PMS2, GPTMS, and TEOS, as illustrated in Figure 4(a), occurs through hydrolysis, condensation, and covalent chemical bonding. Initially, the ester groups (–$COOCH_3$) on the PMMA surface are converted to carboxylic acid groups (–COOH) via acid hydrolysis, increasing the surface reactivity. Subsequently, TEOS and GPTMS undergo hydrolysis (Figure 4(b)), during which their alkoxy groups (–OCH_3 and –OC_2H_5) are replaced by silanol groups (–Si–OH). In the next step (Figure 4(c)), these silanol groups undergo condensation reactions with each other, leading to the formation of siloxane (Si–O–Si) bonds. This process results in a robust silicate network on the particle surface, contributing to structural stability and enhanced surface functionality.

Additionally, as illustrated in Figure 5(a), the epoxy group present in GPTMS can react with the carboxylic acid groups on F-PMS2, forming covalent bonds. Meanwhile, as shown in Figure 5(b), the silanol groups of TEOS and GPTMS can also undergo condensation reactions with the carboxylic acid groups on the F-PMS2 surface, leading to the formation of silicate ester bonds (Si–O–C(=O)–R). This process not only enhances the adhesion of the silicate coating to the F-PMS2 surface but also improves mechanical stability, uniformity, bioactivity, and adhesion to biological tissues. As a result, the combination of siloxane, ester, and covalent linkages yields a robust organic–inorganic hybrid structure with optimized properties for biomedical and tissue engineering applications.

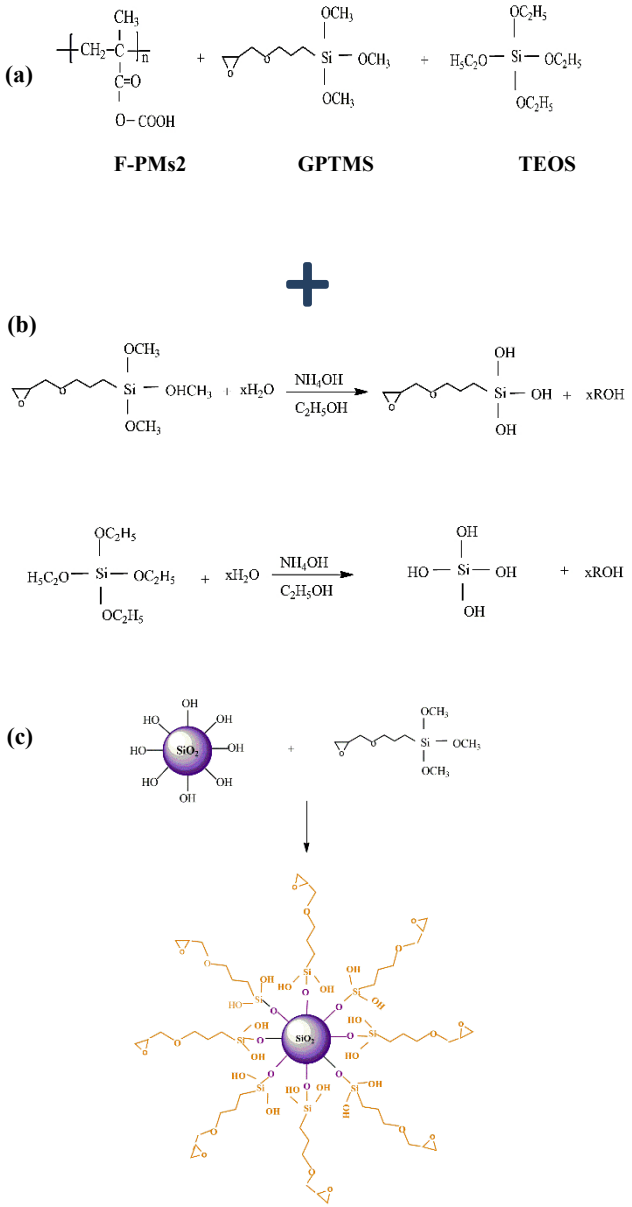

Figure 4. (a) Chemical structures of F-PMs2, GPTMS, and TEOS, (b) hydrolysis-condensation reaction of GPTMS and TEOS, (c) condensation and network formation of GOTMS-TEOS

As the reaction proceeds, F-PMS2 can further interact with the siloxane network formed by GPTMS and TEOS, resulting in the development of a three-dimensional crosslinked network in which F-PMS2 becomes

integrated into the silicate framework. This integration significantly enhances the mechanical strength and thermal stability of the final composite material (Gül et al., 2021).

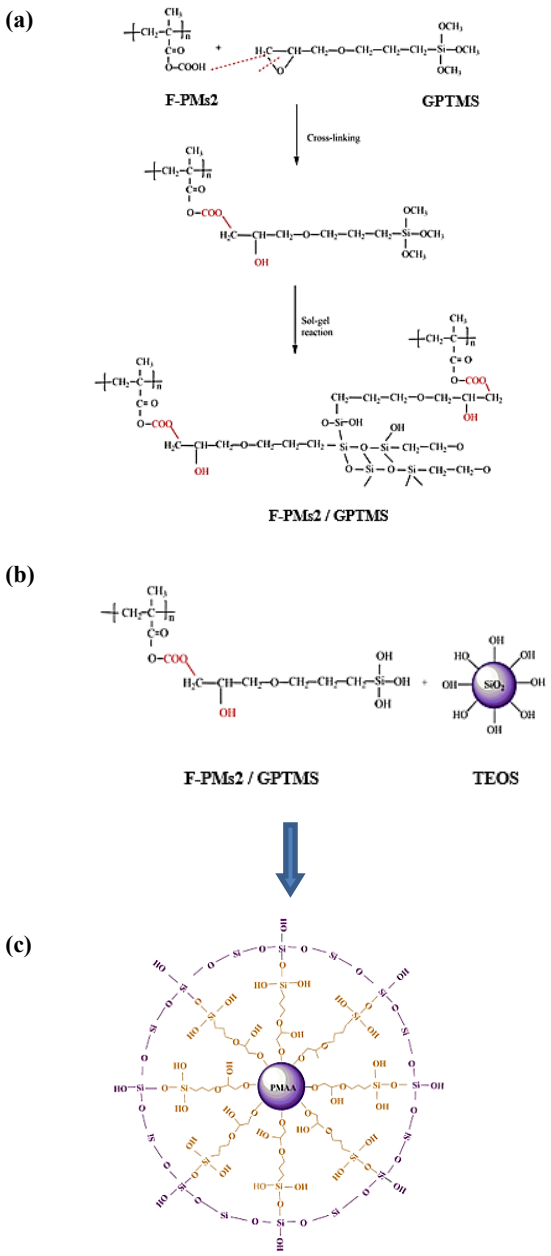

Figure 5. (a) Reaction between GPTMS and F-PMs2, (b) Synthesis reaction of F-PMs2 with GPTMS and TEOS, (c) Proposed schematic of the reaction mechanism between F-PMs2, GPTMS, and TEOS.

3.2.5 FTIR Spectroscopy of F-PMs2 Microspheres Cross-linked with GPTMS and TEOS

To evaluate the functional groups and investigate potential interactions during the surface modification of PMMA microspheres, Fourier Transform Infrared (FTIR) spectroscopy was conducted on various samples, and the results are presented in Figure 6. In the spectrum of the acid-treated sample (F-PMs2), a slight shift in the C–H stretching bands around 2850 cm^{-1} compared to the pure PMs2 was observed, along with the appearance of a broad band in the 3000–3500 cm^{-1} region. This broad absorption is attributed to the formation of hydroxyl groups resulting from the conversion of methyl ester groups to carboxylic acid groups during acid hydrolysis. Additionally, increased intensity in the carbonyl (C=O) bands around 1700–1730 cm^{-1} and broadening of the 1200–1000 cm^{-1} region further support the formation of polar functional groups following acid treatment (Sivakumar & Rao, 2000). In the subsequent chemical surface modification step, two silane agents, GPTMS and TEOS, were employed. GPTMS contains three methoxy groups (–OCH_3) and one epoxy ring (–C–O–C–). In the FTIR spectrum of GPTMS, characteristic CH_3 stretching bands from the methoxy groups appear at ~2943 and 2840 cm^{-1}. Bands at 1193 and 1083 cm^{-1} are attributed to CH_2 vibrations in the glycidoxypropyl chain, while peaks at 1255, 910, and 445 cm^{-1} are associated with the epoxy ring (Ghorbani et al., 2018). TEOS (tetraethyl orthosilicate), on the other hand, contains ethoxy (–OC_2H_5) groups that hydrolyze to form silanol groups (Si–OH), which can further condense to form siloxane bonds (Si–O–Si). In the TEOS spectrum, stretching vibrations of CH_2 and CH_3 from the ethoxy chains appear between 2880–2980 cm^{-1}. Absorption bands in the 1000–1100 cm^{-1} range correspond to Si–O–Si and Si–O–C linkages, while a weak band around 960 cm^{-1} may indicate residual Si–OH bending vibrations.

After applying a combination of GPTMS and TEOS onto the F-PMs2 surface and obtaining the optimized sample (PMS1G2) while maintaining the original morphology, it was expected that hydrolysis of the alkoxy groups would lead to the formation of crosslinked siloxane (Si–O–Si) networks, and that some epoxy groups would react with the surface carboxylic acid groups. However, in the FTIR spectrum of the final sample PMS1G2, distinct and prominent peaks related to silane groups were not clearly visible. This could be due to several factors: (1) the formation of a thin silane coating on the surface, (2) the use of minimal reagent concentrations to preserve microsphere morphology, or (3) overlap of silane-related bands with intrinsic polymer matrix vibrations.

who noted that at lower TEOS concentrations, the intensity of the Si–O–Si peak decreases significantly and may not be detected in FTIR when ultra-thin coatings are present. Additionally, weak signals were observed at ~910, 1255, and 445 cm^{-1}, possibly corresponding to residual epoxy (C–O–C) groups, which may indicate either unreacted GPTMS or the formation of covalent bonds with carboxyl groups on the F-PMs2 surface.

In conclusion, although the formation of a silicate network in PMS1G2 was not directly and strongly reflected in the FTIR spectra, based on the known chemical reactions, relative spectral changes, and

supporting evidence from previous studies, it can be inferred that crosslinking between the silane agents and the modified PMMA surface likely occurred successfully, leading to the formation of the desired organic–inorganic hybrid structure.

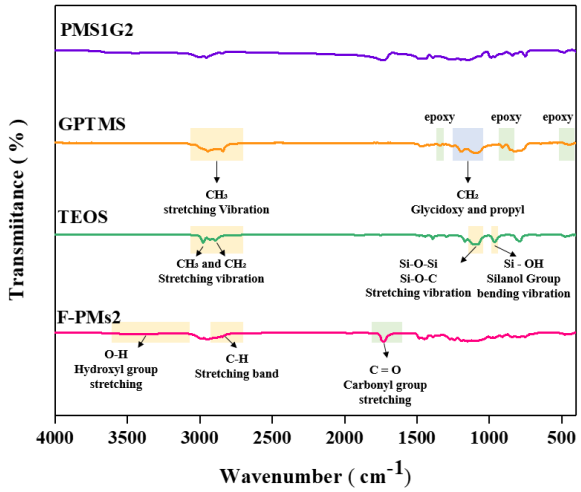

Figure 6. FTIR spectroscopy of F-PMs2, TEOS, GPTMS, and PMS1G2 samples.

3.2.6 Surface Morphology of Silanized Microspheres

Figure 7 shows the FE-SEM images of F-PMS2 microspheres modified with GPTMS. GPTMS is a bifunctional silane containing an epoxy group and three methoxysilane groups (–Si(OCH_3)$_3$), enabling both surface anchoring and self-condensation into a weak siloxane network. The observed particle aggregation may be attributed to van der Waals interactions, GPTMS hydrolysis–condensation behavior, and the absence of a stronger silane source such as TEOS. These forces become more prominent at the micro/nanoscale, leading to partial fusion or clustering of microspheres.

Under basic conditions, the epoxy ring in GPTMS readily opens, while the deprotonation of hydroxyl and carboxyl groups on the F-PMS2 surface enhances nucleophilicity. This facilitates the formation of an ether bond between the epoxy group of GPTMS and the hydroxyl groups on the surface. Additionally, hydrolysis of the methoxy groups in GPTMS generates silanol (–Si–OH) groups, which can further condense into covalent Si–O–Si linkages, reinforcing the surface with an organic–inorganic hybrid structure.

However, excessive condensation of silanols in the absence of TEOS results in uncontrolled siloxane growth and a non-uniform coating. Elemental mapping (EDS-MAP) reveals a heterogeneous distribution of Si, with localized Si-rich domains indicating over-condensation, accompanied by reduced carbon and elevated oxygen levels in these regions. In contrast, areas with minimal Si content show higher carbon presence, reflecting incomplete or absent silane coverage. These inconsistencies in silane distribution adversely affect bioactivity due to surface heterogeneity.

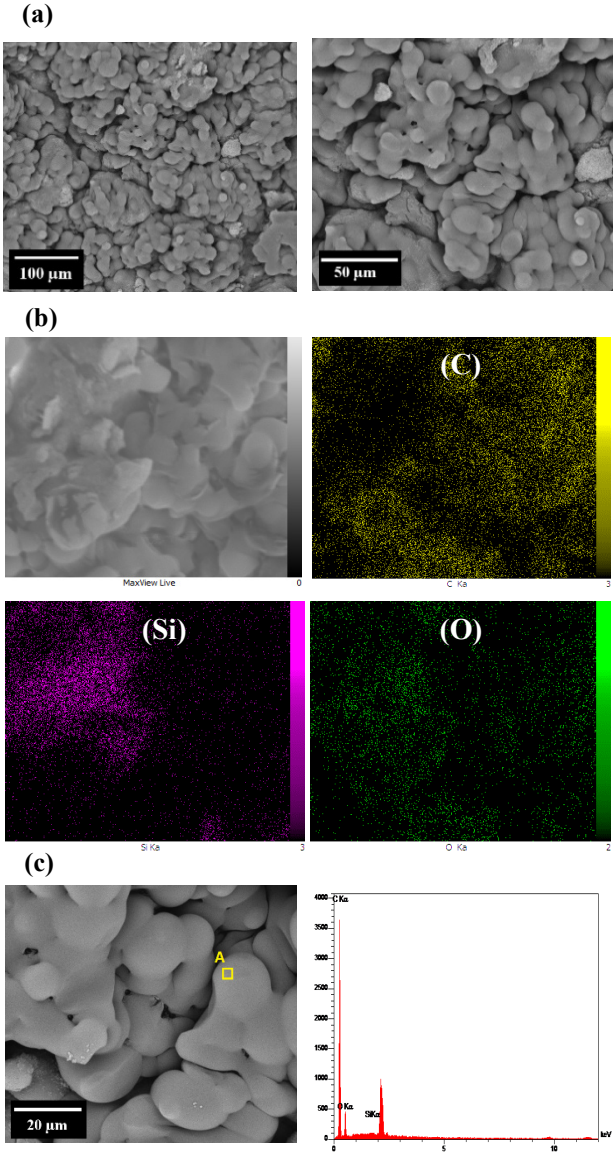

Figure 7. (a) SEM image of PMG, (b) MAP image of PMG, (c) EDS elemental analysis of PMG.

The uneven Si and O elemental maps further confirm the formation of non-uniform siloxane networks. This non-uniformity stems from incomplete or uncontrolled GPTMS hydrolysis and condensation, as reported by Gabrielli et al. (2013), who demonstrated that using GPTMS alone in epoxy–silica hybrid coatings yields inhomogeneous siloxane domains due to incomplete hydrolysis and random condensation of Si–OH groups. They emphasized that the co-utilization of TEOS enhances hydrolysis efficiency and balances the condensation process, resulting in more uniform and stable hybrid coatings. In conclusion, while GPTMS alone contributes to crosslinking, its exclusive use leads to poor coating uniformity and surface heterogeneity.

A combined system of GPTMS and TEOS is therefore recommended to achieve optimized morphology and improved bioactivity of PMMA-based microspheres. In a comparative study (Zhao et al., 2017), three sets of F-PMS2 microspheres were functionalized using varying GPTMS/TEOS ratios to determine the optimal conditions for maintaining spherical morphology, achieving a uniform silicate coating, and enhancing bioactivity. As shown in Figure 8, the base microspheres fabricated via solvent evaporation emulsion exhibited well-defined spherical shapes.

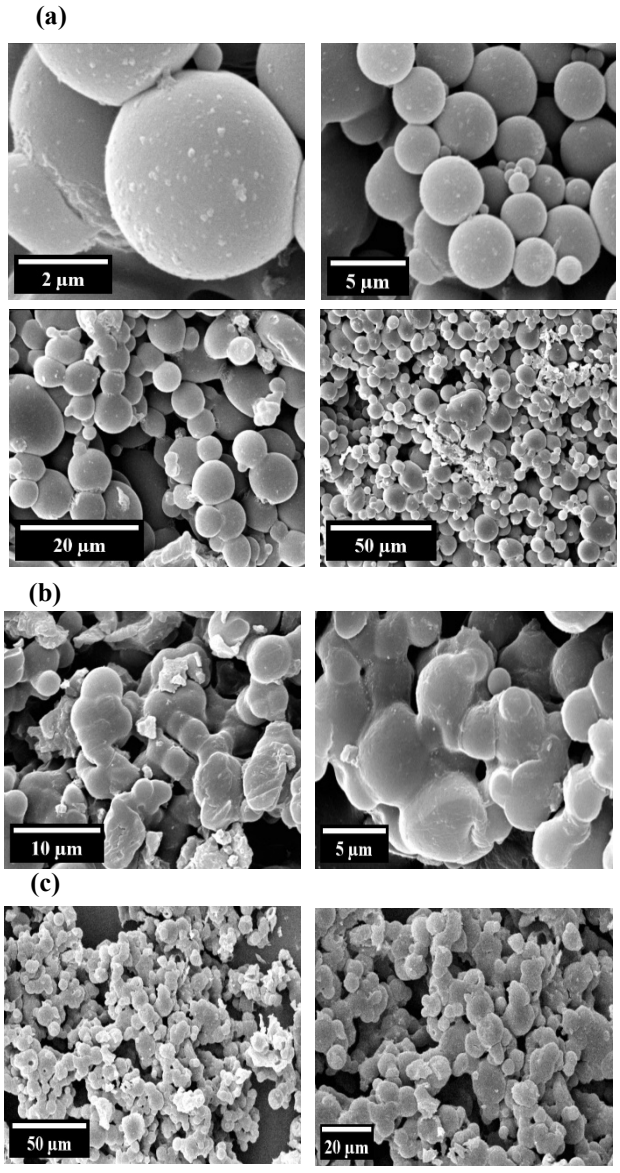

Figure 8. SEM images of the sample: a) containing 1 ml TEOS and 2 ml GPTMS, b) containing 1.5 ml TEOS and 2.5 ml GPTMS, c) containing 2 ml TEOS and 3 ml GPTMS

When the GPTMS/TEOS ratio reached 3:2, excessive silanization occurred, disrupting the spherical structure and causing irregular silica aggregation. These samples displayed rough surfaces and bulky domains, indicating uncontrolled silicate deposition. At a ratio of 2.5:1.5, spherical integrity was better preserved; however, the higher TEOS content still led to thicker coatings and some surface roughness due to localized condensation. The optimal condition was observed at a 2:1 ratio (GPTMS/TEOS), where a balance between silicate deposition and morphological integrity was achieved. This concentration resulted in uniform surface coverage, minimal roughness, and preservation of spherical geometry, making it the most favorable for enhanced surface bioactivity and application in biomedical coatings.

The purpose of EDS and elemental mapping (MAP) was to evaluate the presence and spatial distribution of key elements, including silicon (Si), oxygen (O), and carbon (C), on the surface of silanized F-PMS2 microspheres, in order to assess the uniformity and effectiveness of the silicate coating. As shown in Figure 9, at a high GPTMS/TEOS ratio (PMS2G3), EDS results indicated excessive and heterogeneous silicon content. Elemental maps revealed localized regions with high silicon concentration, corresponding to dense and non-uniform silicon dioxide clusters. In these regions, carbon levels dropped significantly, indicating complete coverage by thick silicate layers, which impeded EDS detection of the underlying polymer surface. The simultaneous increase in oxygen confirmed excessive Si–O–Si bond formation, likely caused by uncontrolled condensation reactions.

At a medium ratio (PMS1.5G2.5), the Si distribution was more balanced, and the overall Si content decreased compared to the high-ratio sample. Nevertheless, localized silica aggregation was still present. Slightly higher carbon levels indicated thinner silicate coatings, although some regions remained fully covered. The O/Si correlation suggested moderate siloxane network formation.

The optimal sample (PMS1G2) exhibited uniform elemental distribution, with no abnormal Si accumulation. The carbon content was higher and more consistent across the surface, indicating thin, well-dispersed silicate coatings. A balanced O/Si ratio further confirmed homogeneous silanization, which is beneficial for ensuring both surface bioactivity and preservation of morphology.

Figure 10, elemental mapping, revealed that in the high-GPTMS/TEOS sample (PMS2G3), the distribution of silicon (Si) and oxygen (O) was highly uneven. Si concentrations were extremely high in some regions and absent in others, indicating uncontrolled silica aggregation.

Correspondingly, oxygen levels were elevated in Si-rich areas, confirming the presence of dense SiO_2 clusters. Such inhomogeneous deposition can hinder the formation of an apatite layer, resulting in poor bioactivity due to reduced surface accessibility and unfavorable surface chemistry.

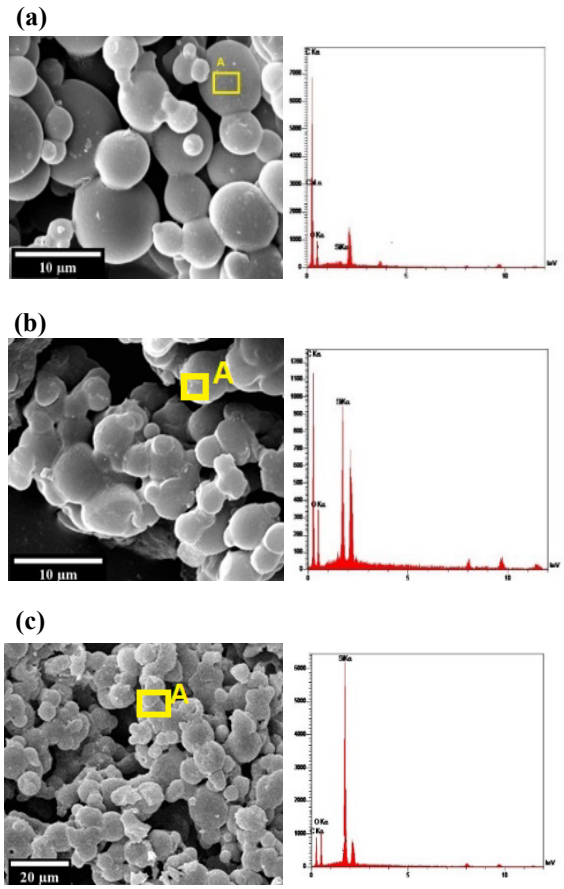

Figure 9. Elemental analysis of the sample containing a) 1 ml TEOS and 2 ml GPTMS, b) 1.5 ml TEOS and 2.5 ml GPTMS, c) 2 ml TEOS and 3 ml GPTMS

TABLE 2. Result of energy-dispersive X-ray spectroscopy (EDS) analysis from the marked points corresponding to Figure 9.

Sample Code	Si	O	C
PMS1G2	2.31	22.14	67.19
PMS2G3	35.27	28.60	22.58
PMS1.5G2.5	27.46	16.61	54.69

In the PMS1.5G2.5 sample, Si distribution was more uniform, though localized aggregation persisted. The strong correlation between Si and O suggested continued formation of Si–O–Si bonds, consistent with partial condensation of the silane network. While this sample demonstrated improved surface coverage compared to the previous one, its bioactivity remained suboptimal.

In contrast, the PMS1G2 formulation exhibited uniform elemental distribution with no excessive Si accumulation. Si and O were evenly dispersed, indicating well-controlled silanization and formation of a homogeneous silicate layer. This structure supported the highest apatite-forming ability and bioactivity, making PMS1G2 the optimal condition for surface modification of F-PMS2 microspheres.

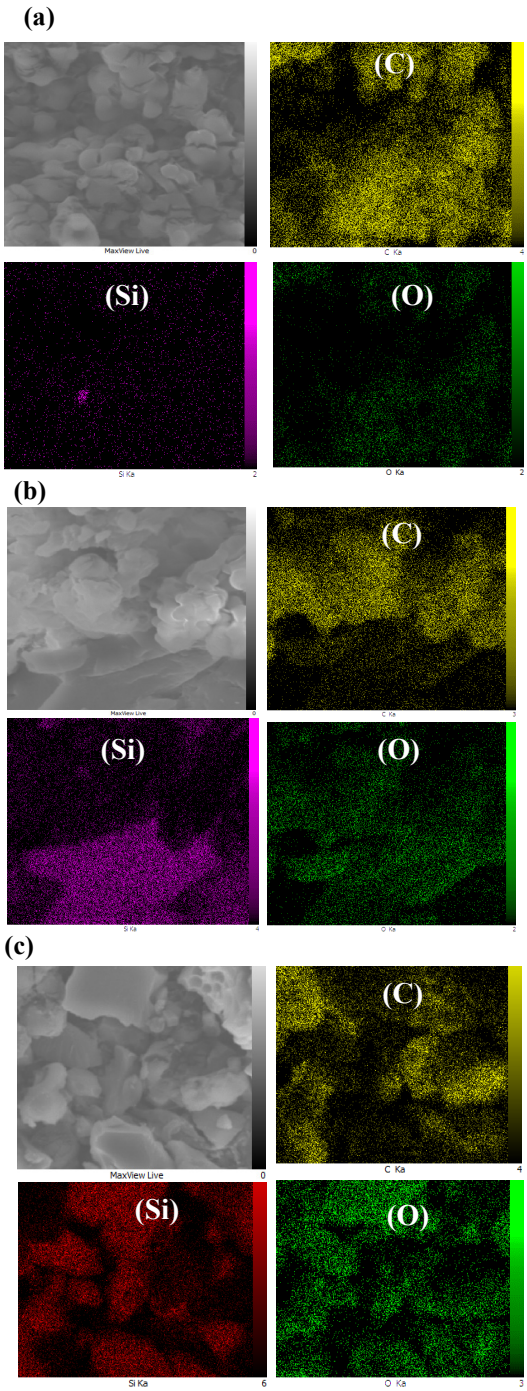

Figure 10. Elemental distribution maps obtained from the sample containing a) 1 ml TEOS and 2 ml GPTMS, b) 1.5 ml TEOS and 2.5 ml GPTMS, and c) 2 ml TEOS and 3 ml GPTMS.

3.2.7 Calcium Phosphate Deposition and Bioactivity Evaluation

Bioactivity refers to the ability of a material to interact with the biological environment and induce specific cellular responses, particularly the formation of hydroxyapatite (HA), a mineral phase similar to the inorganic component of bone. In this study, hybrid

microspheres (PMS1G2) were immersed in simulated body fluid (SBF) to evaluate their apatite-forming ability. The bonding ability to bone is commonly assessed by examining the material's capacity to induce apatite formation on its surface in SBF, which mimics the ionic composition of human blood plasma (Kokubo & Takadama, 2006).

In Figure 11, to investigate surface changes, elemental composition, and mineralization behavior, scanning electron microscopy (SEM) was employed before and after immersion in SBF. SEM analysis provides insights into the surface morphology, apatite crystal growth, and the distribution of key elements within the mineral layer. Before SBF immersion, the surface of PMS1G2 appeared relatively smooth and homogeneous, with minor surface porosity likely resulting from the crosslinking process involving GPTMS and TEOS. No crystalline structures were observed, indicating that apatite was absent from the surface prior to soaking.

After immersion, fine amorphous calcium phosphate particles were detected on the surface, marking the onset of apatite nucleation. These particles tended to aggregate in specific regions, particularly around functional groups such as –COOH and Si–OH, which promote interaction with Ca^{2+} and PO_4^{3-} ions in the SBF solution. After two weeks of immersion, SEM images revealed a uniformly distributed hydroxyapatite (HA) crystalline layer, often appearing as nanoscale spherical or plate-like structures, resembling natural bone apatite. Additionally, increased surface porosity and roughness were observed at this stage, indicating significant HA growth, which is favorable for cell attachment and enhanced biocompatibility.

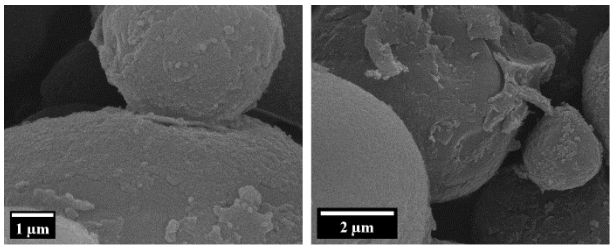

Figure 11. Image of hydroxyapatite deposited on the PMS1G2 microsphere powder

FTIR spectroscopy was employed to investigate the bioactivity process and apatite layer formation after the samples were immersed in simulated body fluid (SBF), as shown in Figure 12. In the control sample (PMS2), which lacked silicate groups and surface modification, no indication of apatite-related or mineral structure bands was observed after immersion in SBF. The FTIR spectrum mainly exhibited the primary polymeric bands.

In contrast, the modified sample PMS1G2, which contains silanol (Si–OH) and carboxylic (–COOH) groups, exhibited significant spectral changes following SBF immersion. An increase in the intensity of bands within the 1080–1150 cm^{-1} region, attributed to Si–O–Si groups, along with a decrease in bands corresponding to Si–OH in the 950–1000 cm^{-1} region, indicates densification of the silicate network and the onset of crosslinking. In addition, broad bands observed in the 3200–3600 cm^{-1} range and the appearance of peaks around 560–600 cm^{-1} and 1430–1450 cm^{-1} suggest the initiation of apatite nucleation and possible formation of an amorphous or early-stage carbonated apatite phase. Although distinct phosphate (P–O) and carbonate (CO_3^{2-}) bands were not resolved, the spectral changes imply the initiation of bioactivity, mineral ion uptake, and suitable conditions for the growth of a bioactive mineral layer on PMS1G2. The absence of well-defined mineral peaks could be attributed to the short immersion time, low amount of deposited mineral, or the presence of poorly crystalline initial phases that have not yet fully crystallized. the PMS1G2 sample also exhibited increased intensity in the 3200–3600 cm^{-1} region, along with phosphate absorption features near 560–600 cm^{-1}, indicating the onset of hydroxyapatite formation after SBF exposure. These findings confirm the critical role of GPTMS in surface activation and induction of bioactivity. Even without fully resolved PO_4^{3-} bands, the hybrid GPTMS structure enhances apatite-forming ability and bioactivity. These results align well with previous studies, demonstrating that surface modification with GPTMS significantly enhances the bioactivity of PMMA microspheres.

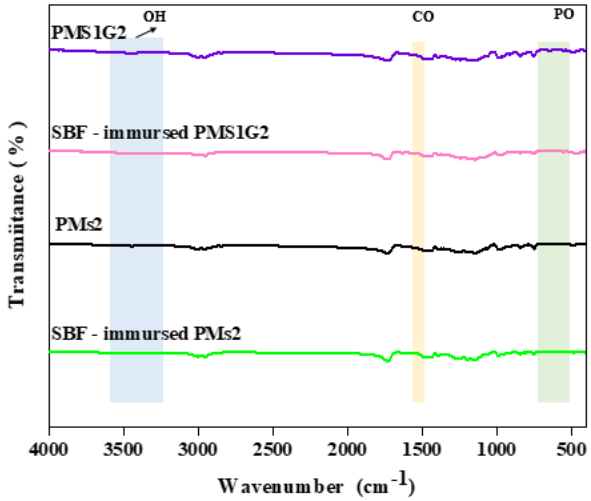

Figure 12. FTIR spectra of PMs2 and PMS1G2 microsphere samples before and after immersion in SBF solution.

X-ray diffraction (XRD) analysis was employed to confirm the bioactivity process and identify apatite phase formation and changes in crystallinity, as illustrated in Figure 4-13. The XRD results indicate that the unmodified PMS2 microspheres exhibit a completely amorphous structure. Due to the absence of bioactive functional groups such as –OH and –COOH, these samples fail to nucleate or grow apatite after immersion

in simulated body fluid (SBF). Consequently, no significant changes in the XRD pattern were observed, confirming the lack of bioactivity in pure PMS2.

In contrast, the silane-modified samples with GPTMS and TEOS developed an amorphous silicate surface layer that acts as active sites for the adsorption of Ca^{2+} and PO_4^{3-} ions, providing favorable conditions for the formation of calcium phosphate phases. After immersion in SBF, distinct peaks appeared at 32.25° and 46.71°, corresponding to the (211) and (222) crystalline planes of hydroxyapatite (HA), respectively. The emergence of these peaks, especially pronounced in the PMS1G2 sample, indicates the onset of HA crystallization and confirms the enhanced bioactivity of the surface-modified microspheres. The relatively low intensity and broadening of these peaks may be attributed to the thin apatite layer or the relatively short immersion time. Nevertheless, the observed changes in the XRD patterns demonstrate that chemical surface modification of PMS1G2 provides an effective route for improving bioactivity and apatite-forming ability.

Detection of apatite crystallization by XRD in SBF-immersed samples can sometimes be challenging because HA may form as a very thin or amorphous layer, or preferred crystal orientation may reduce peak intensities. Therefore, despite the absence of sharp HA peaks, the presence of specific component peaks in FTIR and surface structural changes, particularly in PMS1G2, serves as indirect confirmation of apatite formation and indicates acceptable bioactivity.

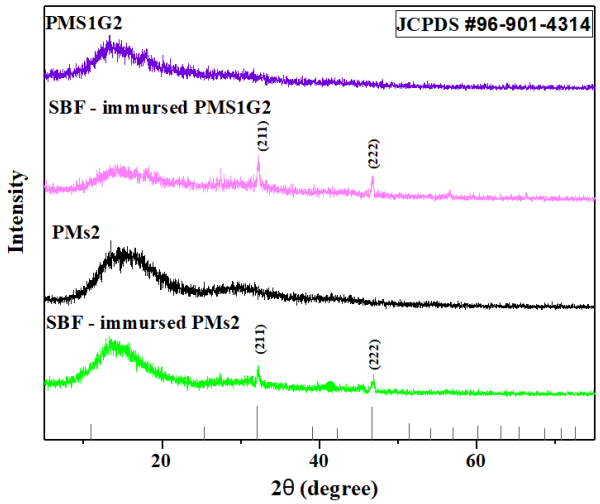

Figure 13. XRD patterns of PMs2 and PMS1G2 microsphere samples before and after immersion in SBF solution.

4. CONCLUSION

This study used the solvent evaporation emulsion method to obtain uniform, spherical, and non-agglomerated particles. Surface modification with sulfuric acid prepared the microspheres for silanization, although excessive treatment led to surface degradation or reduced functional group uniformity. Effective functionalization at an optimized ratio resulted in uniform surface modification, stable bonding, and the formation of a silane network structure, while preserving the spherical morphology of the particles. Although apatite formation confirmed bioactivity in the simulated environment, further cellular-level studies, such as osteoblast differentiation and bone-related gene expression, have not yet been conducted, representing a significant limitation.

REFERENCES

1. Aquino, L. R. C., SILVA, C. C. d., Sombra, A. S., & MACÊDO, A. A. M. (2016). Bone cement: a review. https://repositorio.ufma.br/jspui/handle/123456789/913
2. Clarke, B. (2008). Normal bone anatomy and physiology. Clinical journal of the American Society of Nephrology, 3(Supplement_3), S131-S139. http://doi.org/10.2215/CJN.04151206
3. Gabrielli, L., Russo, L., Poveda, A., Jones, J. R., Nicotra, F., Jiménez-Barbero, J., & Cipolla, L. (2013). Epoxide opening versus silica condensation during sol–gel hybrid biomaterial synthesis. Chemistry–A European Journal, 19(24), 7856-7864. http://doi.org/10.1002/chem.201204326
4. Ghorbani, F., Zamanian, A., Behnamghader, A., & Daliri Joupari, M. (2018). A novel pathway for in situ synthesis of modified gelatin microspheres by silane coupling agents as a bioactive platform. Journal of Applied Polymer Science, 135(41), 46739. https://doi.org/10.1002/app.46739
5. Gül, C., Albayrak, S., Durmuş, H., & Çömez, N. (2021). Characterization of SiO_2 sol-gel coated Ti_6Al_4V alloy obtained by using TEOS and GPTMS. *Science of Sintering, 53*(4), 461-473. https://doi.org/10.2298/SOS2104461G
6. Heinrich, H. T., Bremer, P. J., Daughney, C. J., & McQuillan, A. J. (2007). Acid−Base Titrations of Functional Groups on the Surface of the Thermophilic Bacterium Anoxybacillus flavithermus: Comparing a Chemical Equilibrium Model with ATR-IR Spectroscopic Data. Langmuir, 23(5), 2731-2740. https://doi.org/10.1021/la062401j
7. Hosseini, S., Ibrahim, F., Djordjevic, I., & Koole, L. H. (2014). Recent advances in surface functionalization techniques on polymethacrylate materials for optical biosensor applications. Analyst, 139(12), 2933-2943. http://doi.org/10.1039/C3AN01789C
8. Kokubo, T., & Takadama, H. (2006). How useful is SBF in predicting in vivo bone bioactivity? Biomaterials, 27(15), 2907-2915. https://doi.org/10.1016/j.biomaterials.2006.01.017
9. Loi, F., Córdova, L. A., Pajarinen, J., Lin, T.-h., Yao, Z., & Goodman, S. B. (2016). Inflammation, fracture and bone repair. Bone, 86, 119-130. https://doi.org/10.1016/j.bone.2016.02.020
10. Mashhadian, A., Afjoul, H., & Shamloo, A. (2022). An integrative method to increase the reliability of conventional double emulsion method. Analytica Chimica Acta, 1197, 339523. http://doi.org/10.1016/j.aca.2022.339523
11. Pahlevanzadeh, F., Bakhsheshi-Rad, H., & Hamzah, E. (2018). In-vitro biocompatibility, bioactivity, and mechanical strength of PMMA-PCL polymer containing fluorapatite and graphene oxide bone cements. Journal of the mechanical behavior of biomedical materials, 82, 257-267. http://doi.org/10.1016/j.jmbbm.2018.03.016
12. Pletincx, S., Marcoen, K., Trotochaud, L., Fockaert, L.-L., Mol, J. M., Head, A. R., Hauffman, T. (2017). Unravelling the chemical influence of water on the PMMA/aluminum oxide hybrid interface in situ. Scientific reports, 7(1), 13341. https://doi.org/10.1038/s41598-017-13549-z

13. Singh, B., Singh, P., Sutherland, A. J., & Pal, K. (2017). Control of shape and size of poly(lactic acid) microspheres based on surfactant and polymer concentration. Materials Letters, 195, 48-51. https://doi.org/10.1016/j.matlet.2017.02.068

14. Sivakumar, M., & Rao, K. P. (2000). Synthesis and characterization of poly(methyl methacrylate) functional microspheres. *Reactive and functional polymers, 46*(1), 29-37. https://doi.org/10.1016/S1381-5148(00)00033-X

15. Teimouri, R., Abnous, K., Taghdisi, S. M., Ramezani, M., & Alibolandi, M. (2023). Surface modifications of scaffolds for bone regeneration. Journal of Materials Research and Technology, 24, 7938-7973. https://doi.org/10.1016/j.jmrt.2023.05.076

16. Wang, F., Zhang, Y., Li, X., Wang, B., Feng, X., Xu, H., Sui, X. (2020). Cellulose nanocrystals-composited poly(methyl methacrylate) encapsulated n-eicosane via a Pickering emulsion-templating approach for energy storage. Carbohydrate Polymers, 234, 115934. http://doi.org/10.1016/j.carbpol.2020.115934

17. Zhao, Z.-B., Tai, L., Zhang, D.-M., & Jiang, Y. (2017). Facile fabrication of siloxane@poly(methylacrylic acid) core-shell microparticles with different functional groups. Journal of Nanoparticle Research, 19, 1-9. https://doi.org/10.1007/s11051-017-3777-y